Comparison of the structures and mechanisms of the pistol and hammerhead ribozymes

Timothy J. Wilson, Yijin Liu, Nan Sheng Li, Qing Dai, Joseph A. Piccirilli and David M. J. Lilley

Supplementary Information

FIGURES

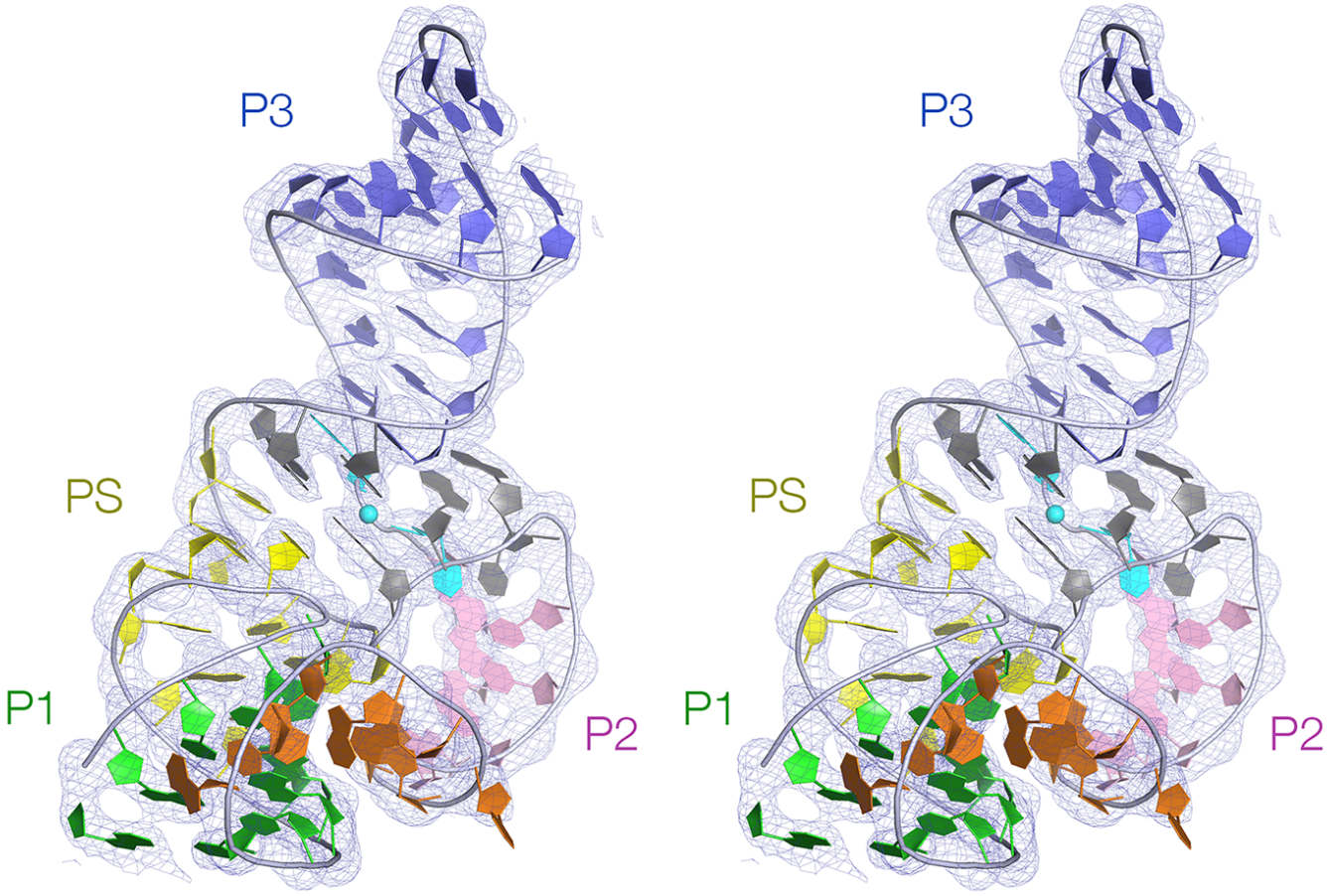

Figure S1. The crystal structure of the pistol ribozyme. A parallel-eye stereoscopic view is shown, with the $2\mathbf{F}_o$-$\mathbf{F}_c$ electron density map contoured at 2 σ. The scissile phosphate is shown as a cyan sphere, and the flanking nucleotides (-1 and +1 positions) are also cyan.

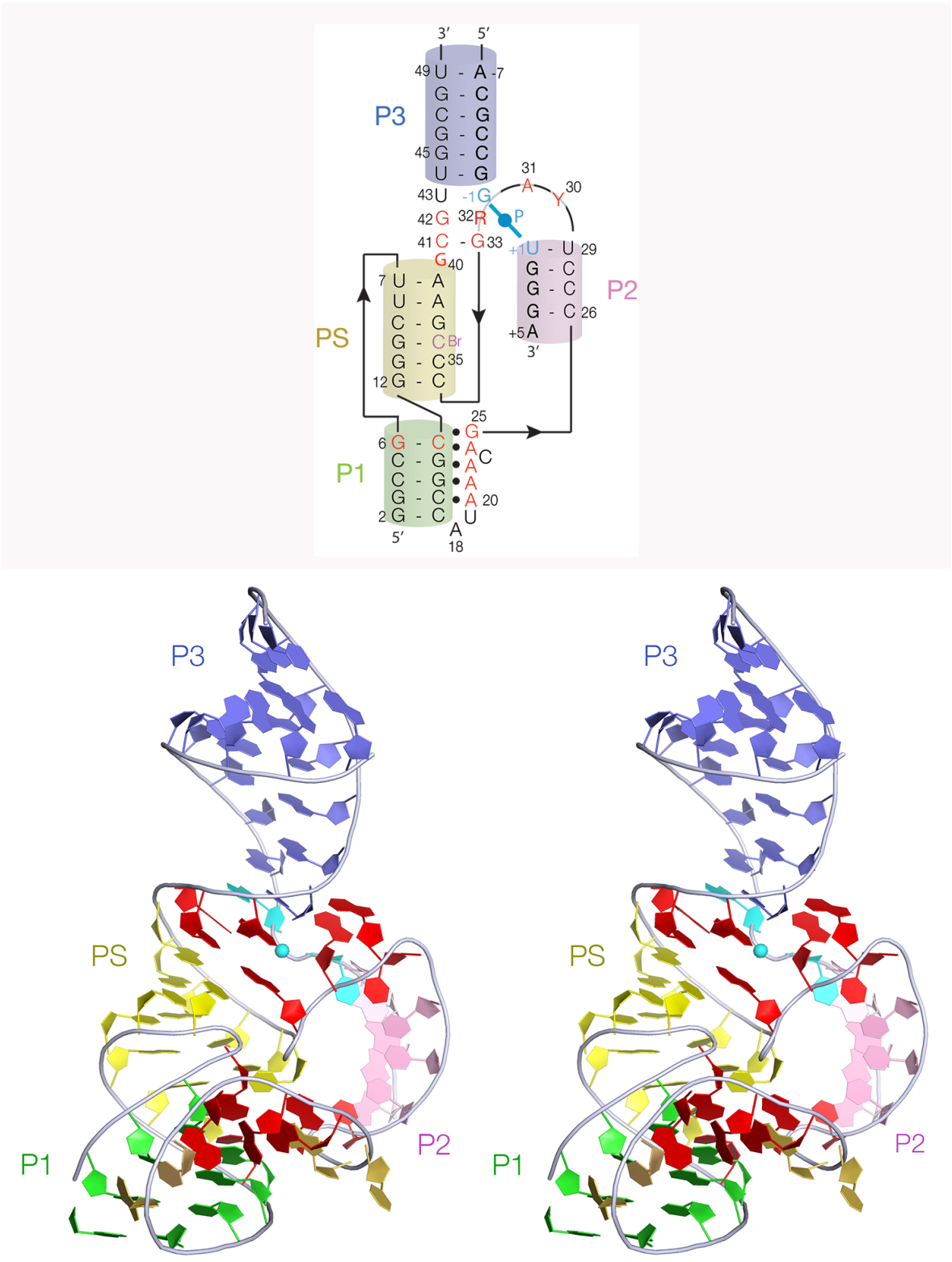

Figure S2. The crystal structure of the pistol ribozyme with the conserved nucleotides highlighted in red. The top shows the secondary structure as it relates to the three-dimensional structure in the crystal. The molecular graphics (lower) is shown in parallel-eye stereoscopic view. Note the conserved nucleotides form two clusters. One is in the junction region around the scissile phosphate i.e. the active center of the ribozyme. The other is in the region of helix P1 and its minor groove interaction, shown in detail in Figure S3.

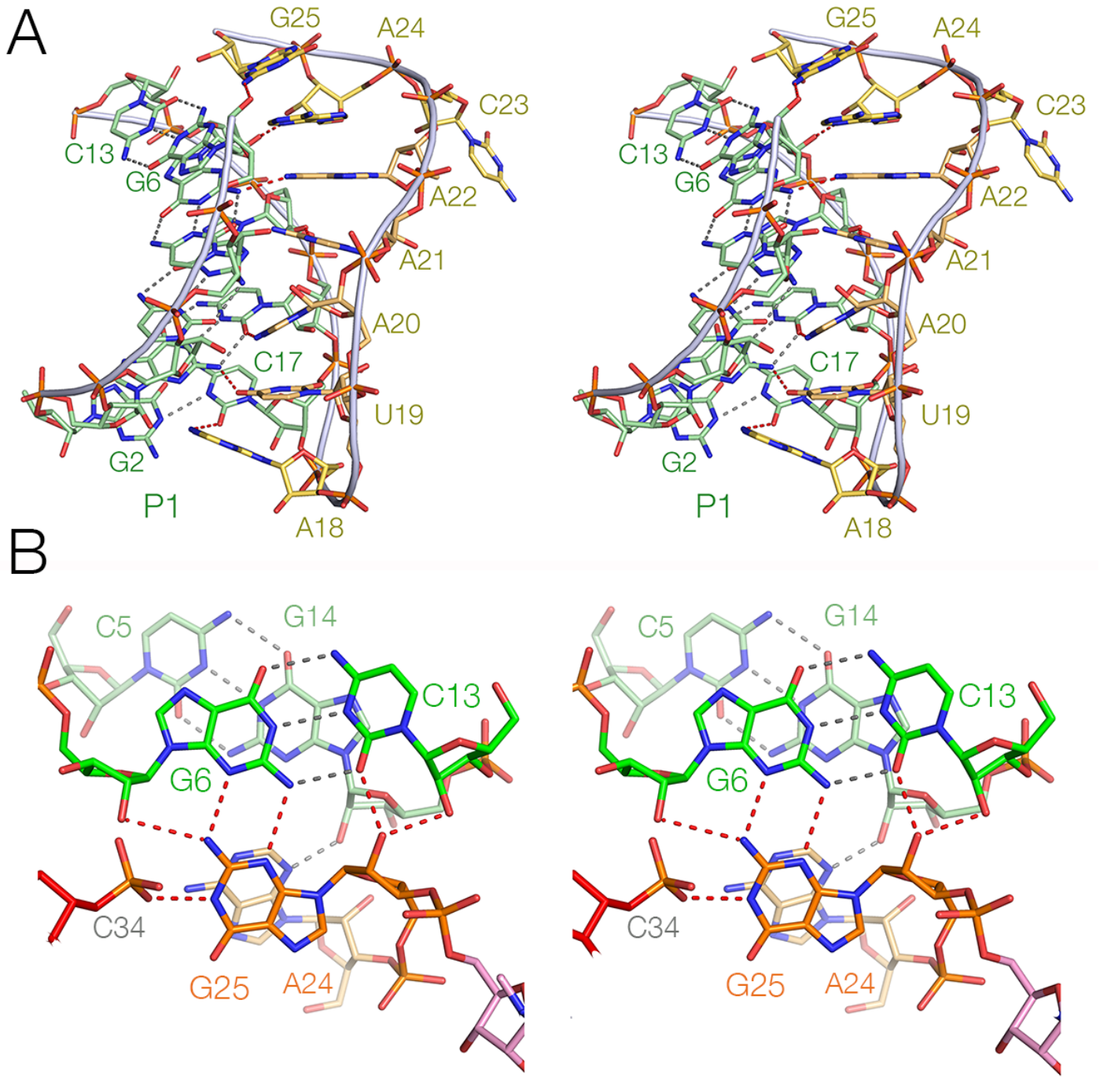

Figure S3 A and B. The linker joining P1 and P2. This linker is clearly important with a run of three highly conserved adenine nucleotides (A20-A22) plus A24 all of which make interactions in the minor groove of P1 (part **A**). These are separated by the bulged out nucleotide at position 23 that is usually a pyrimidine. G25 has a critical role in the structure, making five hydrogen bonds to the conserved base pair G6:C13 and a sixth hydrogen bond to the *pro*R non-bridging oxygen atom of C34 (part **B**). It thus stabilizes the structure at the junction between P1 and PS. Parts **C** and **D** follow.

C

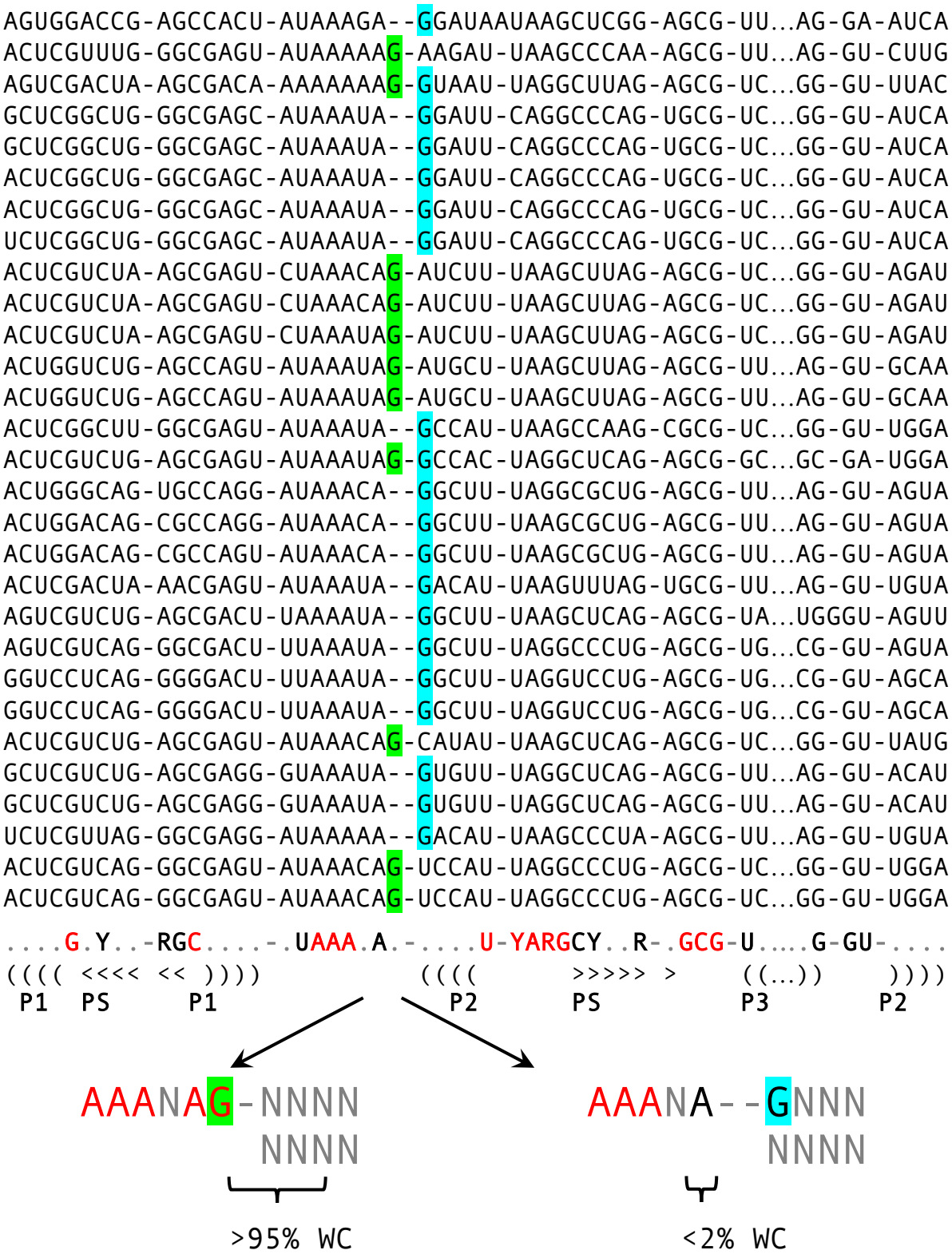
AGUGGACCG-AGCCACU-AUAAAGA--GGAUAAUAAGCUCGG-AGCG-UU...AG-GA-AUCA
ACUCGUUUG-GGCGAGU-AUAAAAAG-AAGAU-UAAGCCCAA-AGCG-UU...AG-GU-CUUG
AGUCGACUA-AGCGACA-AAAAAAAG-GUAAU-UAGGCUUAG-AGCG-UC...GG-GU-UUAC
GCUCGGCUG-GGCGAGC-AUAAAUA--GGAUU-CAGGCCCAG-UGCG-UC...GG-GU-AUCA
GCUCGGCUG-GGCGAGC-AUAAAUA--GGAUU-CAGGCCCAG-UGCG-UC...GG-GU-AUCA
ACUCGGCUG-GGCGAGC-AUAAAUA--GGAUU-CAGGCCCAG-UGCG-UC...GG-GU-AUCA
ACUCGGCUG-GGCGAGC-AUAAAUA--GGAUU-CAGGCCCAG-UGCG-UC...GG-GU-AUCA
UCUCGGCUG-GGCGAGC-AUAAAUA--GGAUU-CAGGCCCAG-UGCG-UC...GG-GU-AUCA
ACUCGUCUA-AGCGAGU-CUAAACAG-AUCUU-UAAGCUUAG-AGCG-UC...GG-GU-AGAU
ACUCGUCUA-AGCGAGU-CUAAACAG-AUCUU-UAAGCUUAG-AGCG-UC...GG-GU-AGAU
ACUCGUCUA-AGCGAGU-CUAAAUAG-AUCUU-UAAGCUUAG-AGCG-UC...GG-GU-AGAU
ACUGGUCUG-AGCCAGU-AUAAAUAG-AUGCU-UAAGCUUAG-AGCG-UU...AG-GU-GCAA
ACUGGUCUG-AGCCAGU-AUAAAUAG-AUGCU-UAAGCUUAG-AGCG-UU...AG-GU-GCAA
ACUCGGCUU-GGCGAGU-AUAAAUA--GCCAU-UAAGCCAAG-CGCG-UC...GG-GU-UGGA
ACUCGUCUG-AGCGAGU-AUAAAUAG-GCCAC-UAGGCUCAG-AGCG-GC...GC-GA-UGGA
ACUGGGCAG-UGCCAGG-AUAAACA--GGCUU-UAGGCGCUG-AGCG-UU...AG-GU-AGUA
ACUGGACAG-CGCCAGG-AUAAACA--GGCUU-UAAGCGCUG-AGCG-UU...AG-GU-AGUA
ACUGGACAG-CGCCAGU-AUAAACA--GGCUU-UAAGCGCUG-AGCG-UU...AG-GU-AGUA
ACUCGACUA-AACGAGU-AUAAAUA--GACAU-UAAGUUUAG-UGCG-UU...AG-GU-UGUA
AGUCGUCUG-AGCGACU-UAAAAUA--GGCUU-UAAGCUCAG-AGCG-UA...UGGGU-AGUU
AGUCGUCAG-GGCGACU-UUAAAUA--GGCUU-UAGGCCCUG-AGCG-UG...CG-GU-AGUA
GGUCCUCAG-GGGGACU-UUAAAUA--GGCUU-UAGGUCCUG-AGCG-UG...CG-GU-AGCA
GGUCCUCAG-GGGGACU-UUAAAUA--GGCUU-UAGGUCCUG-AGCG-UG...CG-GU-AGCA
ACUCGUCUG-AGCGAGU-AUAAACAG-CAUAU-UAAGCUCAG-AGCG-UC...GG-GU-UAUG
GCUCGUCUG-AGCGAGG-GUAAAUA--GUGUU-UAGGCUCAG-AGCG-UU...AG-GU-ACAU
GCUCGUCUG-AGCGAGG-GUAAAUA--GUGUU-UAGGCUCAG-AGCG-UU...AG-GU-ACAU
UCUCGUUAG-GGCGAGG-AUAAAAA--GACAU-UAAGCCCUA-AGCG-UU...AG-GU-UGUA
ACUCGUCAG-GGCGAGU-AUAAACAG-UCCAU-UAGGCCCUG-AGCG-UC...GG-GU-UGGA
ACUCGUCAG-GGCGAGU-AUAAACAG-UCCAU-UAGGCCCUG-AGCG-UC...GG-GU-UGGA
....G.Y..-RGC....-.UAAA.A.-....U-YARGCY..R-.GCG-U.....G-GU-....
((((<<<< <<)))) ((((>>>>> > ((...))))))
P1 PS P1 P2 PS P3 P2
AAANAG-NNNN
NNNN
AAANA--GNNN
NNNN
>95% WC
<2% WC

D

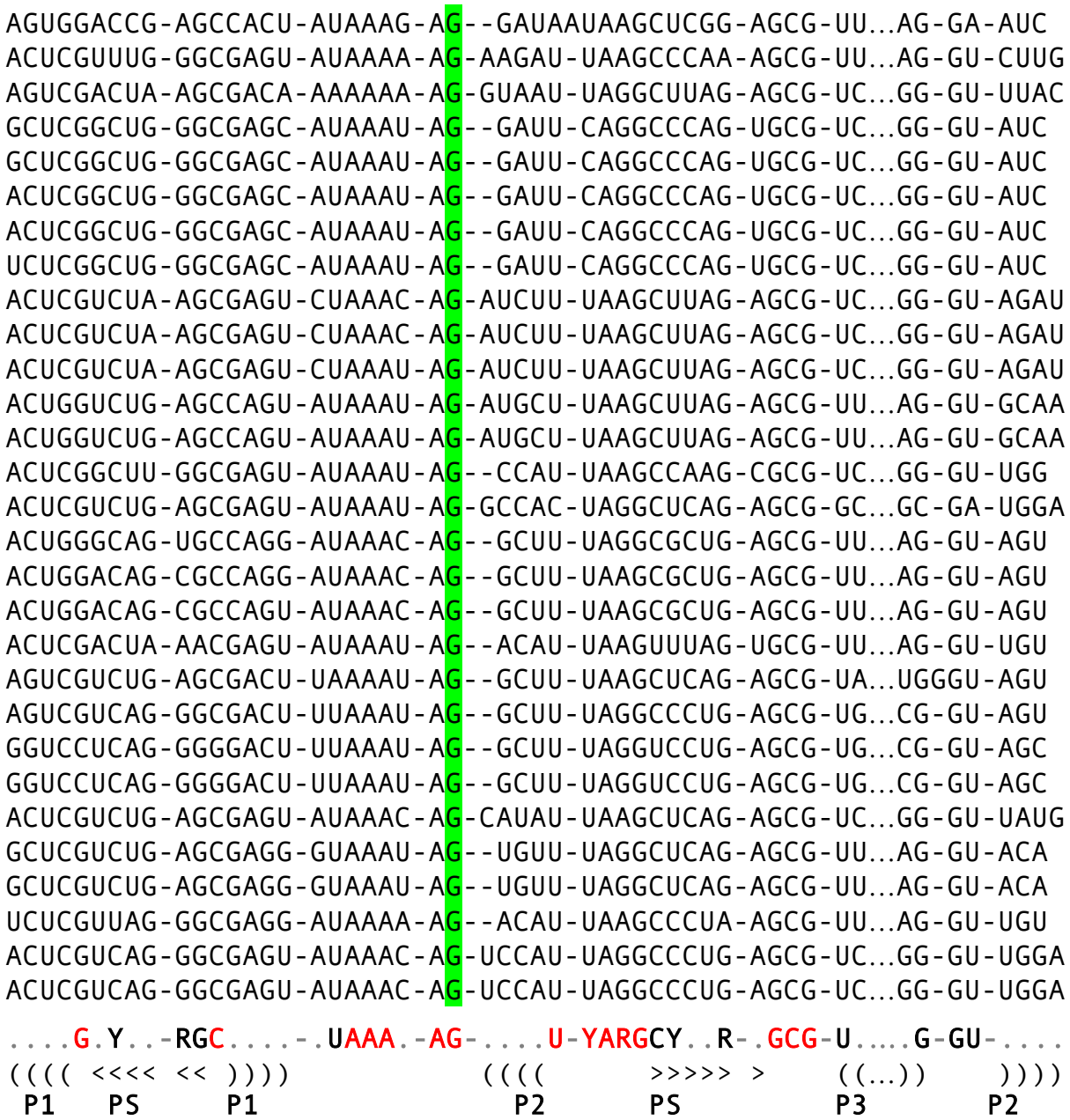

Figure S3. The linker joining P1 and P2. This linker is clearly important with a run of three highly conserved adenine nucleotides (A20-A22) plus A24 all of which make interactions in the minor groove of P1 (part **A**). These are separated by the bulged out nucleotide at position 23 that is usually a pyrimidine. G25 has a critical role in the structure, making five hydrogen bonds to the conserved base pair G6:C13 and a sixth hydrogen bond to the *pro*R non-bridging oxygen atom of C34 (part **B**). It thus stabilizes the structure at the junction between P1 and PS. However in the alignment published by Weinberg *et al.* [1] it is not shown as conserved because it was assigned two alternative positions. This is illustrated by the section of the alignment shown in part **C**. In the column to the right of A24, G is found in 26 % of the sequences (highlighted green), A 1.6% and no nucleotide for the remaining sequences. However, when there is no nucleotide in that position there is almost always a G (highlighted blue) assigned as the first nucleotide in P2. Below the alignment we show the secondary structure and the consensus sequence for the full alignment of 676 sequences,

with nucleotides better than 97% conserved colored red and nucleotides better than 90% conserved colored black. For convenience only the first two base pairs of P3 are shown. The sequences can be separated into two classes with four or three base pairs in P2, depending on the position of G25. In the class with G25 adjacent to A24 the four base pairs in P2 each have greater than 95% Watson-Crick pairing. In contrast, for the class with G as the first nucleotide in P2 this is opposed by C in fewer than 2 % of cases Thus the two classes each have a highly conserved AG sequence and differ in the length of the P2 helix. This variation in the length of P2 is observed in the crystal structures. Our structure has three Watson-Crick base pairs in P2 whereas the other two structures have four [2-3]. We tested the effect of helix length by deleting U26 from the construct we used for cleavage assays. This deletion would be expected to reduce P2 to three base pairs while leaving G25 free to form the base triple with G6:C13. This deletion had no significant effect on activity (Table 1). In contrast deletion of G25 caused a 34-fold decrease in activity, consistent with its important role in the structure. Part **D** presents a revised alignment for the sequences in part **C** incorporating variability in the length of P2. A revised alignment for all sequences is also provided in Stockholm format (pistol_ribozyme.sto). Parts **A** and **B** are shown as parallel-eye stereoscopic images.

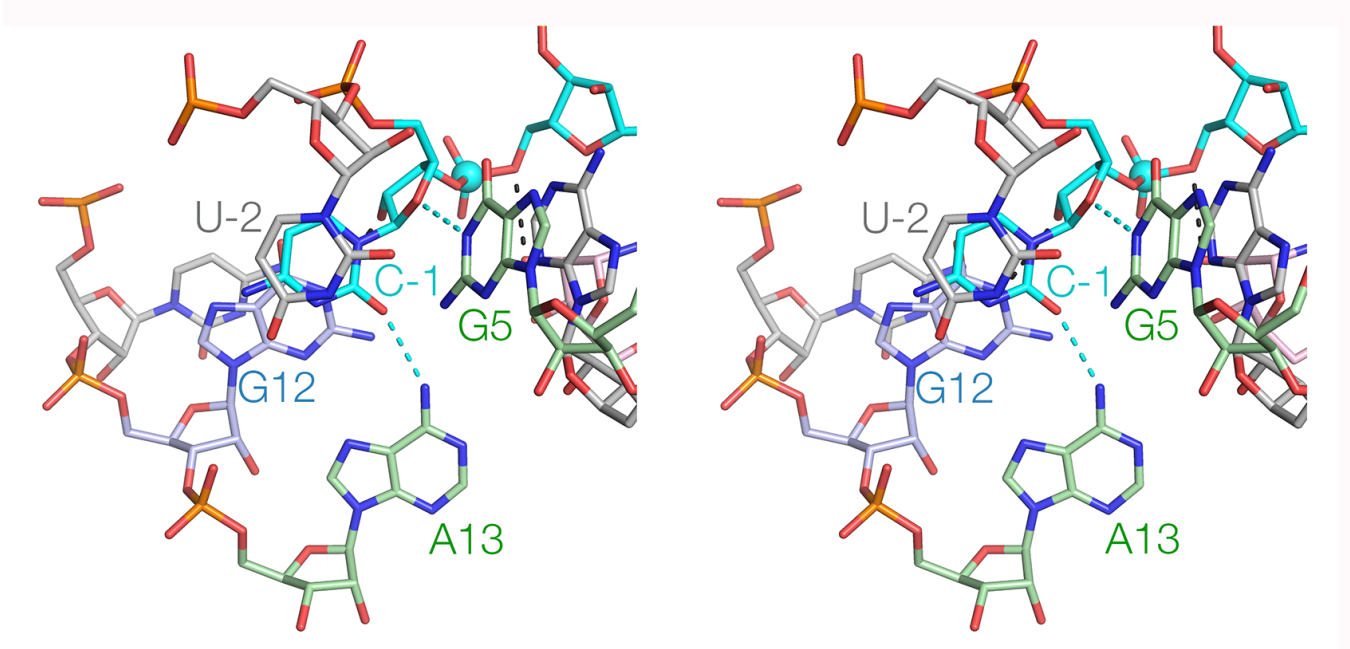

Figure S4. Parallel-eye stereoscopic view of the environment of C-1 in the hammerhead ribozyme. C-1 is stacked between the nucleobases of G12 and U-2 (U16.1 at the end of helix III). Its O2 accepts a hydrogen bond from A13 N6 and its O4' accepts one from G5 N1 (both shown cyan).

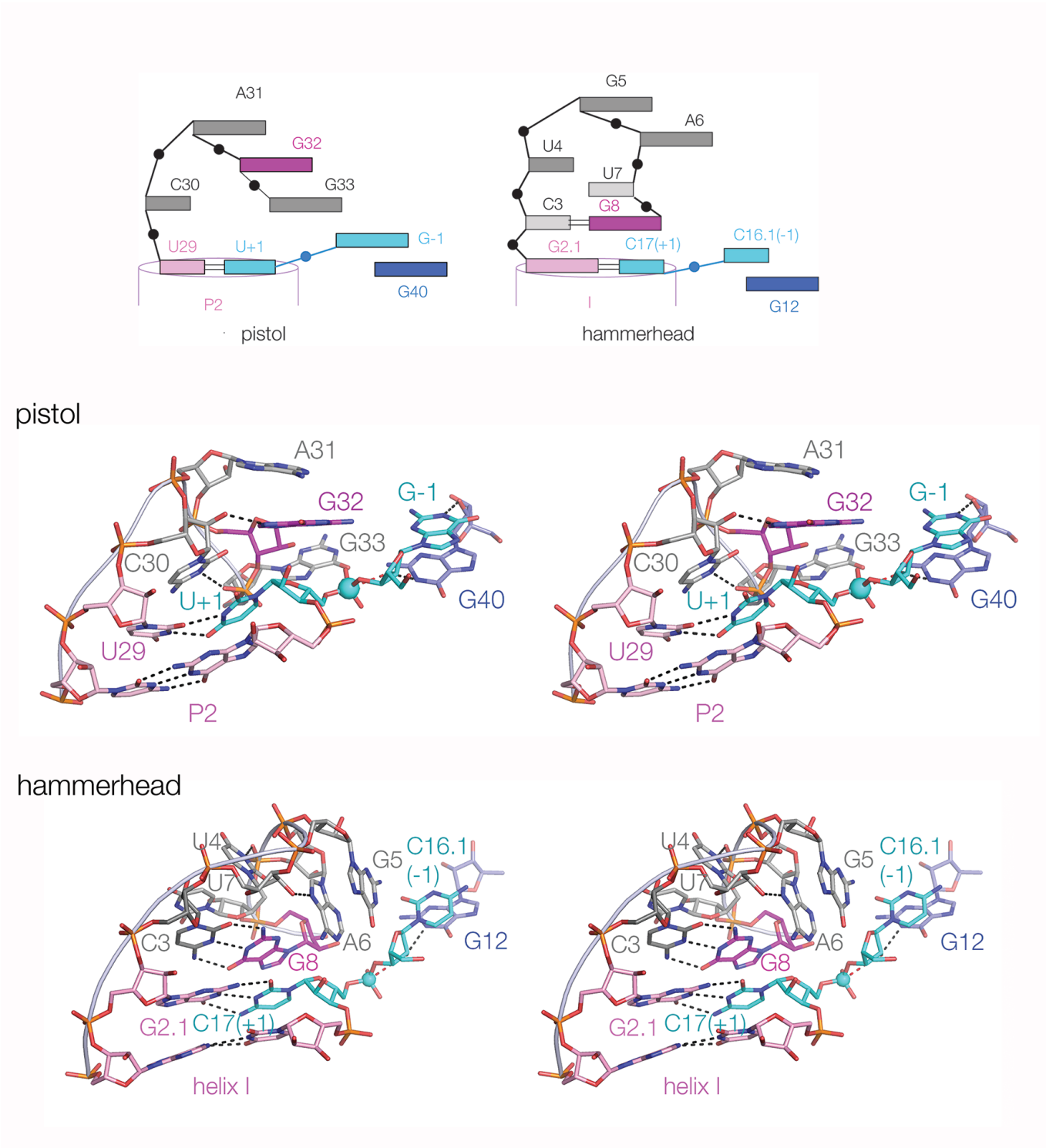

Figure S5. The structures of the turn regions of the pistol and hammerhead ribozymes. Schematic views are shown at the top. Below are shown parallel-eye stereoscopic views of the pistol and hammerhead loop structures, with similar perspectives on the nucleotides flanking the scissile phosphate (cyan in both cases). G40 (pistol) and G12 (hammerhead) are located in a very similar manner, but note the contrasting positioning of the critical G32 and G8 nucleotides.

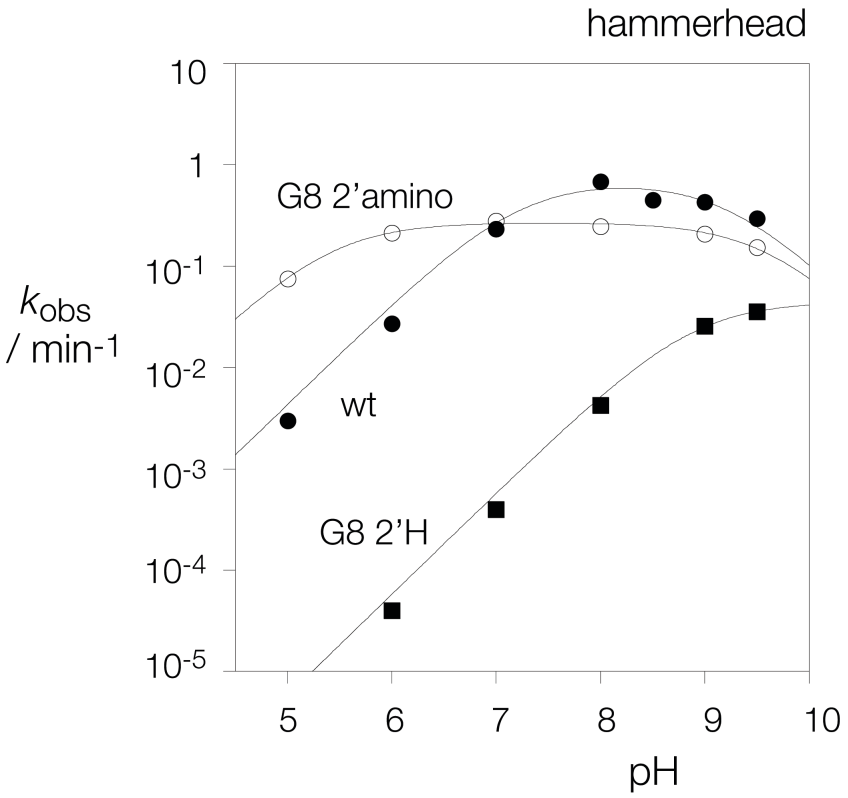

Figure S6. The role of the 2'-hydroxyl group of G8 in the hammerhead ribozyme using atomic mutation. Plot of cleavage rate as a function of reaction pH performed for the unmodified ribozyme (filled circles), G8 2'NH_2 ribozyme (open circles) and G82'H ribozyme (filled squares) in the presence of 1 mM Mg^{2+} and 2 M Na^+ ions. Equivalent data have been obtained in the presence of 2 M Na^+ ions in Figure 4. The data for the unmodified and G8 2'NH_2 ribozymes were fitted using equation 2, giving apparent pK_a values of 7.2 and 9.2 for the unmodified ribozyme and 5.4 and 9.6 for the G8 2'NH_2 ribozyme. The data for the G8 2'H ribozyme were fitted using equation 1, giving an apparent pK_a value of 8.9.

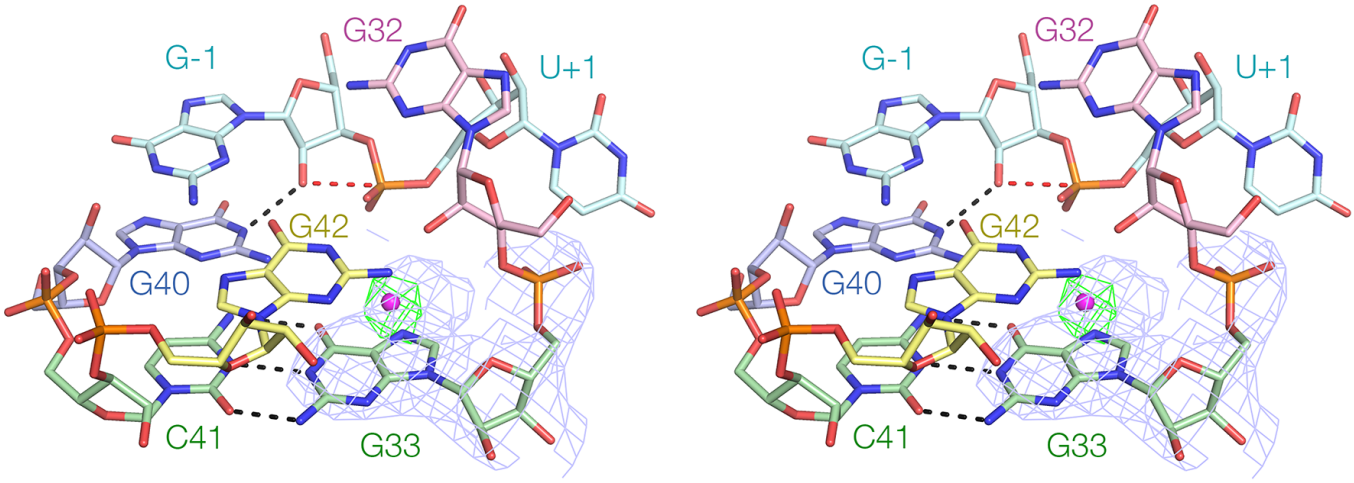

Figure S7. A metal ion binding site close to the active center of the pistol ribozyme. A parallel-eye stereoscopic view is shown. The light blue mesh shows the $2F_o$-F_c electron density contoured at 2σ in the vicinity of G33. The crystals were soaked with 1 mM $MnCl_2$, and excited with X-rays close to the peak of anomalous scatter for Mn^{2+}. The green mesh shows the resulting F_o-F_c anomalous peak contoured at 7σ.

TABLE

Crystal	Pistol ribozyme
Data collection	
Wavelength / Å	0.9686
Resolution range / Å	62.22 – 3.1 (3.21 – 3.1)
Space group	P 6_1
Unit cell	94.31, 94.31,96.03 Å
	$\alpha, \beta=90°, \gamma=120°$
Total reflections	34088 (6230)
Unique reflections	8853 (1592)
Multiplicity	3.9 (3.9)
Completeness /%	99.70 (99.4)
$< I/\sigma (I) >$	9.4 (1.5)
R-merge	0.060 (0.884)
CC1/2	0.971 (0.604)
Refinement	
R-work	0.1759
R-free	0.1802
Number of atoms	
RNA	1368
ligands	23
rmsd	
Bond lengths /Å	0.007
Bond angles / °	1.04
Average B-factor	137.45
Macromolecules	137.19
ligands	150.31
solvent	151.29
PDB	6R47

Statistics for the highest resolution shell are in parenthesis.

Table S1 Details of data collection and refinement statistics for the data as deposited in the PDB.

References

1. Weinberg, Z.; Kim, P. B.; Chen, T. H.; Li, S.; Harris, K. A.; Lunse, C. E.; Breaker, R. R., New classes of self-cleaving ribozymes revealed by comparative genomics analysis. *Nature Chem. Biol.* **2015,** *11* (8), 606-610.
2. Ren, A.; Vusurovic, N.; Gebetsberger, J.; Gao, P.; Juen, M.; Kreutz, C.; Micura, R.; Patel, D. J., Pistol ribozyme adopts a pseudoknot fold facilitating site-specific in-line cleavage. *Nature Chem. Biol.* **2016,** *12* (9), 702-708.
3. Nguyen, L. A.; Wang, J.; Steitz, T. A., Crystal structure of Pistol, a class of self-cleaving ribozyme. *Proc. Natl. Acad. Sci. USA* **2017,** *114* (5), 1021-1026.